

Hierarchical structure and dynamics of an ionic liquid 1-octyl-3-methylimidazolium chloride

Osamu Yamamuro, Takeshi Yamada, Maiko Kofu, Masamichi Nakakoshi, and Michihiro Nagao

Citation: *J. Chem. Phys.* **135**, 054508 (2011); doi: 10.1063/1.3622598

View online: <http://dx.doi.org/10.1063/1.3622598>

View Table of Contents: <http://jcp.aip.org/resource/1/JCPSA6/v135/i5>

Published by the [American Institute of Physics](#).

Related Articles

Vibrational energy transfer and anisotropy decay in liquid water: Is the Förster model valid?
J. Chem. Phys. **135**, 164505 (2011)

Decoupling charge transport from the structural dynamics in room temperature ionic liquids
J. Chem. Phys. **135**, 114509 (2011)

A polarizable ion model for the structure of molten CuI
J. Chem. Phys. **134**, 044501 (2011)

The low frequency dynamics of supercooled LiBr, 6H₂O
J. Chem. Phys. **134**, 034514 (2011)

Structural study of low concentration LiCl aqueous solutions in the liquid, supercooled, and hyperquenched glassy states
J. Chem. Phys. **134**, 024515 (2011)

Additional information on *J. Chem. Phys.*

Journal Homepage: <http://jcp.aip.org/>

Journal Information: http://jcp.aip.org/about/about_the_journal

Top downloads: http://jcp.aip.org/features/most_downloaded

Information for Authors: <http://jcp.aip.org/authors>

ADVERTISEMENT

**AIP**Advances

Submit Now

**Explore AIP's new
open-access journal**

- **Article-level metrics
now available**
- **Join the conversation!
Rate & comment on articles**

Hierarchical structure and dynamics of an ionic liquid 1-octyl-3-methylimidazolium chloride

Osamu Yamamuro,^{1,a)} Takeshi Yamada,¹ Maiko Kofu,¹ Masamichi Nakakoshi,²
and Michihiro Nagao^{3,4}

¹*Institute for Solid State Physics, University of Tokyo, 5-1-5 Kashiwanoha, Kashiwa, Chiba 277-8581, Japan*

²*Instrumental Analysis Center, Yokohama National University, 79-1 Tokiwadai, Hodogaya-ku, Yokohama 240-8501, Japan*

³*NIST Center for Neutron Research, National Institute of Standards and Technology, 100 Bureau Drive, Gaithersburg, Maryland 20899-6102, USA*

⁴*Center for Exploration of Energy and Matter, Indiana University, Bloomington, Indiana 47408-1398, USA*

(Received 21 March 2011; accepted 6 July 2011; published online 3 August 2011)

We have performed the heat capacity, neutron diffraction, and neutron quasielastic scattering measurements of an ionic liquid 1-octyl-3-methylimidazolium chloride (C8mimCl). The heat capacity data revealed that C8mimCl exhibits a glass transition with a large heat capacity jump at $T_g = 214$ K, which is lower than T_g of C4mimCl with a shorter alkyl-chain. In the neutron diffraction measurement for a deuterated analogue, d-C8mimCl, the peaks associated with the inter-domain, inter-ionic, and inter-alkyl-chain correlations appeared at (3, 11, and 14) nm⁻¹, respectively. The temperature dependence of these peaks indicates that the packing of the alkyl-chains becomes more compact and the domains become more vivid and larger as decreasing temperature. The quasielastic neutron scattering measurements using neutron spin echo and time-of-flight type instruments demonstrated that C8mimCl has faster relaxations probably owing to the alkyl-group and a slower relaxation owing to the ions. The latter relaxation, which is related to the glass transition, is of non-exponential as in the α relaxation of glass-forming molecular liquids. The relaxation of domains could not be observed in the present experiment but should have relaxation times longer than 100 ns. This is the first report to clarify temperature dependence of the hierarchical structure and relaxations simultaneously for a typical ionic liquid. © 2011 American Institute of Physics. [doi:10.1063/1.3622598]

I. INTRODUCTION

Ionic compounds usually have melting temperatures higher than room temperature because of their strong and long-range interionic interaction. However, it was recently found that a series of organic ionic compounds has melting temperatures lower than room temperature and they are called “room temperature ionic liquids” or simply “ionic liquids (ILs).” The cations of ILs are alkylimidazolium, alkylpyridinium, alkylammonium, etc., which consist of core parts with positive electric charges and alkyl-chains with hydrophobic interactions. On the other hand, halogens (Cl⁻, Br⁻, I⁻) and various ionic groups, e.g., BF₄⁻, PF₆⁻, (CF₃SO₃)⁻, (CF₃SO₂)₂N⁻ (TFSI), can be the anions of ILs. The chemical structure of an IL is shown in Fig. 1(a). ILs are remarked as novel green solvents and electrochemical materials with negligible vapor-pressure and combustibility. It is noteworthy that both cations and anions can be designed to produce various physical and chemical properties. A good example is a magnetic ionic liquid C4mimFeCl₄ (C4mim: 1-butyl-3-methylimidazolium) developed by Hayashi and Hamaguchi.¹ It has a large magnetic susceptibility of 5.10×10^{-7} m³g⁻¹ at room temperature.

Compared with application studies using ILs, the basic scientific studies are not so many. However, some of

important physical properties of ILs have already been reported. Our calorimetric studies^{2,3} revealed that most of imidazolium-based ILs exhibit glass transitions around 200 K and their glass transition temperatures T_g s depend on the size of anions; the larger the anion size is, the lower T_g becomes. It is known that the viscosities of ILs roughly reflect their T_g s. The Stokes-Einstein (SE) law is qualitatively valid for the viscosities and dielectric relaxation times of several imidazolium-based ILs.⁴ However, the SE law is invalid for the rotational and conformational relaxations of solute molecules in ILs.⁵ Inhomogeneous structure described below could be important to consider the SE law.

The structures of ILs have been studied by x-ray⁶⁻¹⁰ and neutron^{11,12} diffraction techniques. The local structures of ILs are similar to those in their crystals; the imidazolium-based cations are coordinated by anions to minimize electrostatic energies. The alkyl chain plays an important role to determine the morphology of ILs. Furthermore, it is recently found that ILs have separation between ionic and neutral (alkyl-chain) domains in nanometer length scales.¹³⁻¹⁶ This is also demonstrated by molecular dynamics (MD) simulation studies.^{8,17-19} The spectroscopic studies^{20,21} have revealed that the alkyl-chains have various conformers and their populations change with temperature. Thus the ILs have the hierarchical structures over a wide space range from 0.1 nm

^{a)}Electronic mail: yamamuro@issp.u-tokyo.ac.jp.

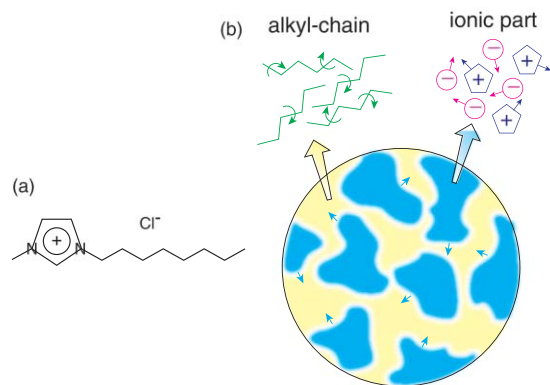


FIG. 1. (a) Chemical structure of C8mimCl. (b) Schematic illustration of a hierarchical structure of ionic liquids.

to 10 nm as schematically shown in Fig. 1(b). Each part may have an individual relaxation time.

The coherent neutron scattering is a powerful tool to investigate the collective dynamics of ILs since one can selectively observe the motion of a definite part of the hierarchical structure by focusing the scattering vector Q . On the other hand, the incoherent neutron scattering enable one to observe selectively the self motion of an atom with large incoherent scattering cross section; e.g., H atoms in cations of ILs. The incoherent quasielastic neutron scattering (QENS) works by Triolo *et al.*^{22,23} demonstrated that a Q - and T -insensitive fast (sub-ps) relaxation and a non-Debye and non-Arrhenius slow relaxation are present as in the case of glass-forming molecular liquids. A recent coherent neutron spin echo (NSE) work²⁴ with a deuterated IL also demonstrated the non-Debye nature of the ionic motions but could not observe the domain motion in ns time range. The dynamics of the domain is a quite unexplored region of the IL research.

The general purpose of our study is to clarify the hierarchical structures and dynamics mentioned above by using various coherent and incoherent neutron scattering techniques. This may contribute to understanding the mechanisms of various characteristic properties of ILs; i.e., low fusion temperatures, validity of the SE law, anion-size dependence of glass transitions, etc. We have already investigated several imidazolium-based ILs with relatively shorter alkyl-chains and various anions. We found that alkyl-chains are highly disordered and moving very fast (in ps order) at room temperature.^{3,25} In the present work, we have taken 1-octyl-3-methylimidazolium chloride (C8mimCl) which has relatively longer alkyl-chains and so may have a clear domain structure. The chemical structure of C8mimCl is shown in Fig. 1(a). We have performed coherent neutron scattering experiments with time-of-flight and spin echo spectrometers to investigate the overall dynamical features of C8mimCl; i.e., the motions of the alkyl-chains, ions, and domains. Calorimetric and neutron diffraction experiments have also been carried out to obtain the information on the phase behavior and the temperature dependence of the hierarchical structure.

II. EXPERIMENTAL

A. Sample preparation

The sample of C8mimCl, whose purity was claimed to be more than 99%, was purchased from Ionic Liquids Technologies GmbH and used in the heat capacity measurement without further purification. For the neutron scattering experiments, deuteration of the sample was required to avoid strong incoherent scattering from hydrogen (H) atoms. The deuterated analogue (d-C8mimCl) was obtained from the reaction of deuterated n-octylchloride and deuterated methylimidazole. The deuteration ratio of the d-C8mimCl is estimated to be $\sim 98\%$ from the deuteration ratios of the starting materials of the synthesis.

B. Heat capacity

The heat capacity measurements were performed with an in-house built adiabatic calorimeter in the temperature range from 5 K to 340 K.²⁶ The sample of 2.513 g was loaded into the copper cell with helium gas which facilitates thermal equilibration inside the cell. The measurement was carried out using a standard intermittent heating method, i.e., repetition of equilibration and energizing intervals. The temperature increment for each measurement was 0.3 K around 5 K and increased with increasing temperature to reach 2.5 K at 200 K. The temperature increment was reduced to smaller than 1 K in the glass transition region. The resolution of the temperature measurement is $\sim 100 \mu\text{K}$ and the heat leakage at adiabatic conditions is smaller than $3 \mu\text{Js}^{-1}$. The accuracy of the heat capacity measurement was better than 1% at $T < 10$ K, 0.5% at $10 \text{ K} < T < 30$ K, and 0.1% at $T > 30$ K.

C. Neutron diffraction

The neutron powder diffraction experiments were performed on the powder diffractometer called HERMES,²⁷ which was constructed by Institute for Materials Research (IMR), Tohoku University. This instrument is installed at the T1-3 port of the JRR-3 reactor in Japan Atomic Energy Agency (JAEA), Tokai, Japan. Neutrons with a wavelength of 0.182 nm, which are obtained by (331) reflection of the Ge monochromator, were used in this instrument. The sample of d-C8mimCl was loaded in a concentric double-cylinder aluminum can (45 mm in height, 18.0 mm in inner diameter of the outer cylinder, 16.0 mm in outer diameter of the inner cylinder). The amount of the sample was 2.1 g corresponding to 1.9 cm^3 in volume and 35 mm in height. The sample can was then sealed by using an indium gasket. This sample can was used also for the quasielastic neutron scattering and neutron spin echo experiments described below. The can was mounted on the cold head of a closed cycle He-gas refrigerator. The sample was cooled down to 190 K and the diffraction data were recorded in the heating direction at (190, 226, 262, 302, and 333) K. The scattering angle 2θ range of the measurements was from 1.3° to 151.2° and the step was 0.1° . The duration of each measurement was 2 h.

D. Neutron spin echo

Neutron spin echo experiments were performed using the NG5-NSE spectrometer^{28,29} at the NIST Center for Neutron Research (NCNR) of National Institute of Standards and Technology (NIST, USA). The spectrometer is installed at the NG5 of the guide hall at the NCNR. The beam line includes a neutron velocity selector to choose a neutron wavelength and a transmission polarizer and a reflection analyzer for the capability of neutron polarization analyses. The wavelength of used neutrons was 0.6 nm with the wavelength resolution of about 20%. The scattering vector Q was chosen at 2.8 nm^{-1} and 11 nm^{-1} to observe selectively the scattering data at the positions of the diffraction peak. The former corresponds to the inter-domain correlation and the latter to the inter-ionic correlation as described later. The data were taken at (244, 262, 280, 298, 315, 333, and 353) K and at Fourier times between 0.007 ns and 15 ns to observe the collective movements at the correlation peaks. The resolution data were taken at 50 K for each Q . The temperature was controlled with a closed cycle refrigerator. The DAVE software package was used to reduce the NSE data from the echo signal to the intermediate scattering function.³⁰

E. Time-of-flight neutron scattering

The QENS data of d-C8mimCl were measured with a time-of-flight spectrometer AGNES (Refs. 31 and 32) of the Institute for Solid State Physics, The University of Tokyo. This instrument is installed at the cold neutron guide (C3-1) of JRR-3. Neutrons with a wavelength of 0.422 nm (for standard mode) or 0.550 nm (for high resolution mode) are extracted with an array of five PG(002) monochromators and pulsed with a double Fermi chopper. The pulsed neutrons are scattered by a sample and detected with 328 ^3He tube detectors arranged in a wide detector bank covering scattering angles of from 10° to 130° . The energy resolution E_{res} , energy range ΔE , and Q range at the standard mode, which was used in this experiment, are $E_{\text{res}} = 120 \mu\text{eV}$, $-4 \text{ meV} < \Delta E < 20 \text{ meV}$, and $2.6 \text{ nm}^{-1} < Q < 27 \text{ nm}^{-1}$, respectively. The quasielastic scattering data were recorded at the same temperatures as in the NSE measurements. The counting time was about 18 h for each temperature.

III. RESULTS AND DISCUSSION

A. Heat capacity

Figure 2 shows the heat capacity of C8mimCl. The heat capacity of C4mimCl (Ref. 2) is plotted together for comparison. A jump of heat capacity corresponding to a glass transition appeared at 214 K, which is lower than the glass transition temperature of C4mimCl ($T_g = 225 \text{ K}$). It is of interest that the substance with longer alkyl-chain (C8mimCl) exhibits lower T_g than that with shorter-alkyl-chain (C4mimCl). This indicates that the T_g of ionic liquids is not dominated simply by the van der Waals interaction among the alkyl-chains. The T_g of ionic liquids could be governed by the balance between the van der Waals and electrostatic

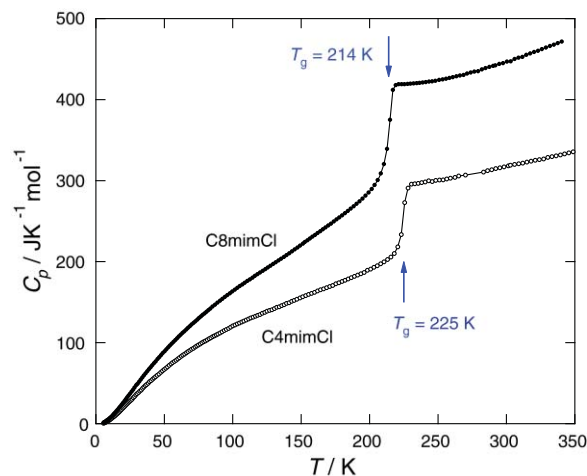


FIG. 2. Heat capacities of C8mimCl and C4mimCl.² The standard deviation of the data is less than 0.1% above 30 K that is much smaller than the plot circles.

interactions of the alkyl and ionic parts forming hierarchical structures. The magnitude of the jump ΔC_p of C8mimCl is larger than that of C4mimCl. This is consistent with usual tendency of ΔC_p in aliphatic glass formers, implying that the excess (configurational) heat capacity above T_g involves the contribution from the ordering/disordering effect of alkyl-chains.

B. Neutron diffraction

Figure 3 shows the neutron diffraction patterns of d-C8mimCl measured by HERMES. Clear peaks appeared at around (3, 11, and 14) nm^{-1} . There have been several diffraction studies reporting the three peaks characteristic to ionic liquids.⁶⁻¹⁶ Annappreddy *et al.*¹⁹ have discussed the origin of

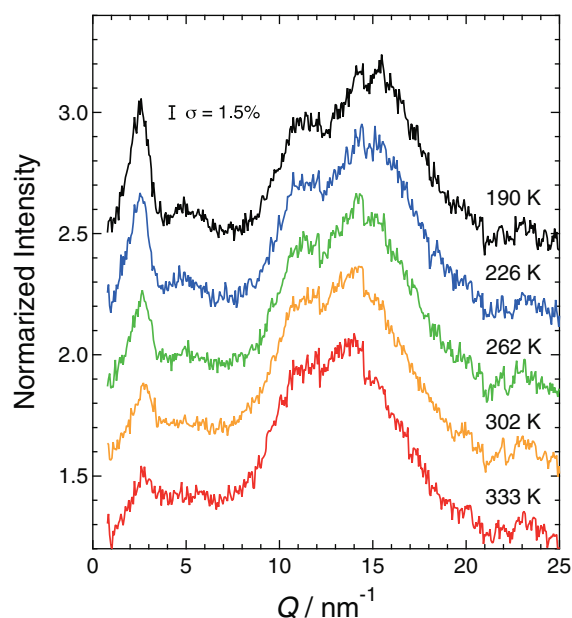


FIG. 3. Neutron diffraction patterns of d-C8mimCl. A vertical bar represents magnitude of standard deviation σ of raw data throughout the paper.

these three peaks based on their molecular dynamics simulation for $C_n\text{mimX}$ ($n = 6, 8, 10, X = \text{Cl}, \text{PF}_6$) which are closely related to our target material C8mimCl . They assert that the 3 nm^{-1} peak is due to the correlation between the polar groups which are separated by the alkyl-chains. This local structure is consistent with the concept of the domains if they have micelle- or lamella-like structure. The 11 nm^{-1} peak (0.9 nm^{-1} peak in their calculation) was assigned to the correlation between the adjacent polar groups. The 14 nm^{-1} peak was described to be associated with various inter atomic correlations. Taking other MD simulation^{8,17–19} and diffraction data^{8–12} into consideration as well, the peaks at 3 nm^{-1} and 11 nm^{-1} observed in this study are considered to be due to the inter-domain and inter-ionic correlations, respectively. Though the 14 nm^{-1} peak may be due to the superimposition of many atomic correlations, the dominant contribution should be due to the inter-alkyl-chain correlation considering the large number of atoms belonging to the alkyl-chains. The coherent neutron scattering cross section of each atom is as follows; D: 5.59 b, C: 6.65 b, N: 11.01 b, Cl: 11.53 b, giving uniform scattering contribution from each atom. Another suggestive information for the 14 nm^{-1} peak is that a peak appears at around 14 nm^{-1} corresponding to the inter-alkyl-chain correlation in the x-ray diffraction data of normal paraffins.³³ Hence, in this paper, the 3 nm^{-1} , 11 nm^{-1} , and 14 nm^{-1} peaks are attributed to the inter-domain, inter-ionic, and inter-alkyl-chain correlations, respectively. The following relaxation data are discussed based on this premise.

As cooling the sample, the position of the inter-ionic peak does not change much while that of the inter-alkyl peaks shifts to the high- Q side. A similar result have been obtained in the neutron diffraction work on C4mimPF_6 by Triolo *et al.*¹² These data indicate that the inter-ionic distance is almost constant while the inter-alkyl distance becomes shorter, corresponding to the compact packing of the alkyl-chains as decreasing temperature. This result is reasonable considering the interaction of each part; i.e., strong Coulomb force for the ions and weak van der Waals force for the alkyl-chains.

To investigate the temperature dependence of the domain peak at 3 nm^{-1} , we have fitted the peaks with Lorentz functions as shown in Fig. 4. The Q range used for the fitting was between 0.9 nm^{-1} and 3.7 nm^{-1} . This is the fitting sometimes performed for first sharp diffraction peaks of liquids or amorphous solids. The parameters determined by the fittings, peak intensities, peak positions, and peak widths, are plotted as functions of temperature in Fig. 5. The peak intensity, reflecting the contrast of the scattering cross sections between alkyl- and ionic-domains, increases with decreasing temperature. The peak position decreases with decreasing temperature, indicating that the size of the domains increases with decreasing temperature. The peak width, which is generally corresponding to the inverse of correlation length, also slightly decreases with decreasing temperature. The present results reveal that the domains become more vivid (ordered) and larger as decreasing temperature. This is the first neutron diffraction data demonstrating clear temperature dependence of IL domains.

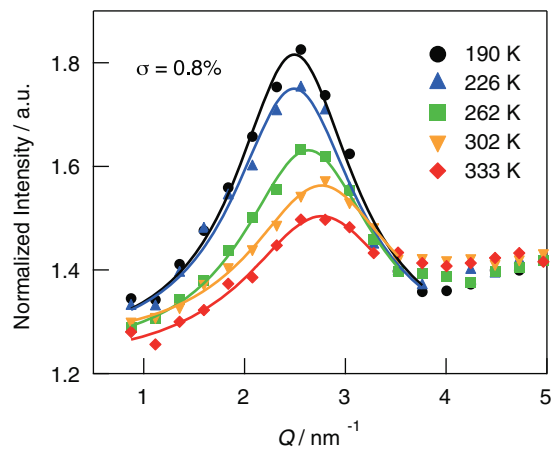


FIG. 4. Neutron diffraction peak corresponding to the inter-domain correlation of d-C8mimCl. The curves represent the results of the fittings with Lorentz functions (see text for the details).

C. Quasielastic neutron scattering

Figures 6 and 7 show the intermediate scattering functions of d-C8mimCl obtained by NSE. The data in Figs. 6 and 7 were recorded at $Q = 11 \text{ nm}^{-1}$ and $Q = 2.8 \text{ nm}^{-1}$, respectively. The data at $Q = 2.8 \text{ nm}^{-1}$ consist mainly of the relaxations of the domains, while those at $Q = 11 \text{ nm}^{-1}$ both of the ionic parts and alkyl-chains. As shown in Fig. 6, there were, at least, two relaxation components depending on temperature. Therefore, the data were fitted to the following equation:

$$I(Q, t) = f \exp\left(-\frac{t}{\tau_{\text{fast}}}\right) + (1 - f) \exp\left[-\left(\frac{t}{\tau_{\text{slow}}}\right)^\beta\right], \quad (1)$$

where the first term is an exponential function corresponding to the faster relaxation and the second term is a stretched exponential (Kohlrausch-Williams-Watts) function

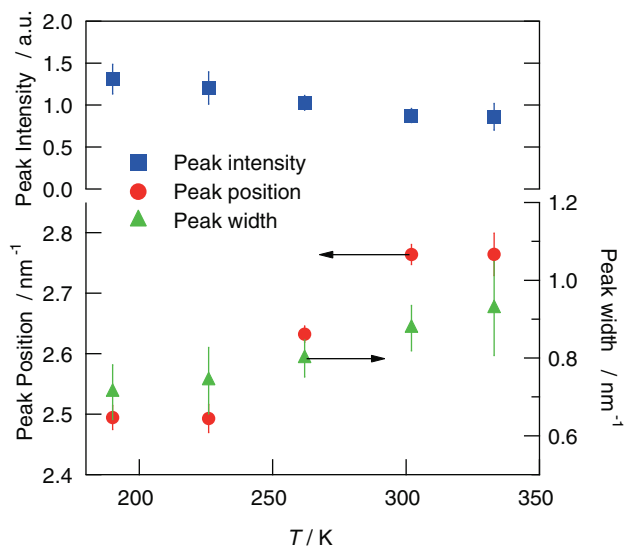


FIG. 5. Temperature dependence of the peak positions, intensities, and widths of the domain peak of d-C8mimCl. Error bars represent standard uncertainty determined by the fitting.

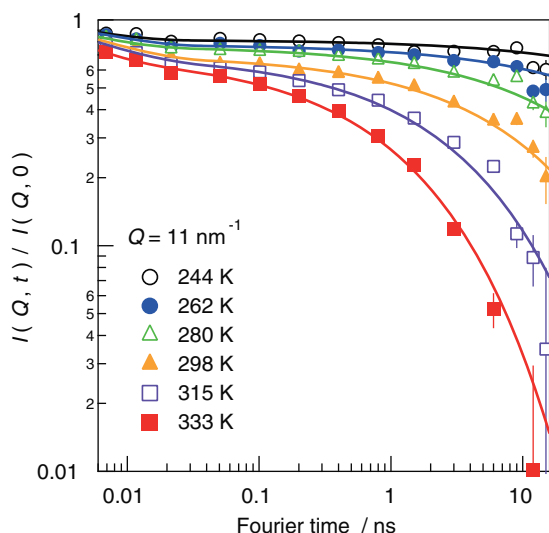


FIG. 6. Intermediate scattering functions of d-C8mimCl observed at $Q = 11 \text{ nm}^{-1}$. Error bars represent standard uncertainty determined by the fitting.

corresponding to the slower relaxation. The parameter f is the fraction of the fast relaxation, τ is the relaxation time, and β is the non-exponential parameter. In the course of the fitting, we noticed that the β determined by the fitting was around 0.5 and did not depend on temperature much. Therefore, we fixed the β to 0.5 and performed the fitting with three adjustable parameters of τ_{fast} , τ_{slow} , and f . The fitting was good as shown in Fig. 6. The present result is consistent with the previous reports by Triolo *et al.* for C4mimPF₆.²² They also found a faster motion reproduced by an exponential function and a slower motion reproduced by a stretched exponential function. The mechanism of each relaxation is discussed in Sec. III D.

Figure 7 shows the intermediate scattering functions at $Q = 2.8 \text{ nm}^{-1}$, which were totally different from those at

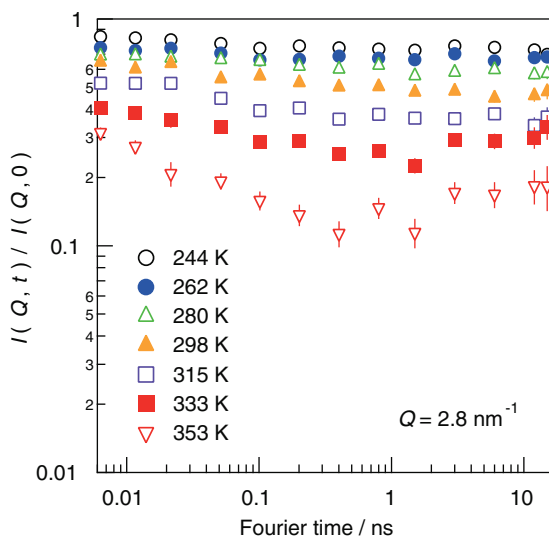


FIG. 7. Intermediate scattering functions of d-C8mimCl observed at $Q = 2.8 \text{ nm}^{-1}$. Error bars represent standard uncertainty determined by the fitting.

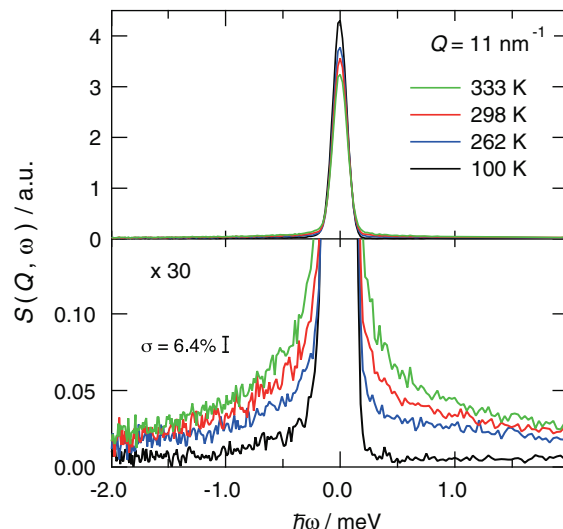


FIG. 8. Dynamic structure factors of d-C8mimCl observed at $Q = 11 \text{ nm}^{-1}$.

$Q = 11 \text{ nm}^{-1}$. Fast relaxations, whose relaxation time is as short as τ_{fast} , were observed in the whole temperature range. After this relaxation, $I(Q, t)$ became almost flat and did not start to relax toward zero even at 15 ns. The present data suggest that the relaxation time of the domain motion is much longer than 100 ns. It is noteworthy that the magnitude of the unrelaxed part has similar temperature dependence as that of the intensity of the domain peak; i.e., they become smaller as increasing temperature. This fact may indicate that the fast relaxation at $Q = 2.8 \text{ nm}^{-1}$ relates to the broken part of the domain but, for further discussion, it is required to make NSE experiments with Fourier times longer than 100 ns or to investigate ILs with faster domain dynamics.

To make further investigation on the fast relaxation mode at $Q = 11 \text{ nm}^{-1}$, the QENS spectra of d-C8mimCl were measured on AGNES at the same temperatures as in the NSE experiment. From the energy resolution of AGNES, it can be regarded that the quasielastic scattering is only due to the fast mode. Figure 8 shows the QENS spectra at each temperature. Each curve is the average of the raw data in the Q region between 10 nm^{-1} and 12 nm^{-1} . These data were fitted to

$$S(Q, \omega) = R(Q, \omega) \otimes [\delta(Q) + L_1(Q, \omega) + L_2(Q, \omega)], \quad (2)$$

where $R(Q, \omega)$ is the resolution function of the AGNES spectrometer, $\delta(Q)$ is the delta function, $L_1(Q, \omega)$ and $L_2(Q, \omega)$ are Lorentz functions, and \otimes represents the operator of the convolution. The fitting was excellent at all temperatures as shown in Fig. 9. To obtain reasonable fitting, two Lorentz functions were required in the AGNES data, while a single exponential function was employed to explain the fast decay in the NSE data. This is because the precision of AGNES is much better than NSE in the time range of 0.01 ns.

The relaxation data measured at higher ($12 \text{ nm}^{-1} < Q < 25 \text{ nm}^{-1}$) and lower ($5 \text{ nm}^{-1} < Q < 10 \text{ nm}^{-1}$) Q ranges were almost the same as those at $Q = 11 \text{ nm}^{-1}$, suggesting that the fast motion is of a local mode. Unfortunately, the fast relaxation observed at $Q = 2.8 \text{ nm}^{-1}$ in NSE could not

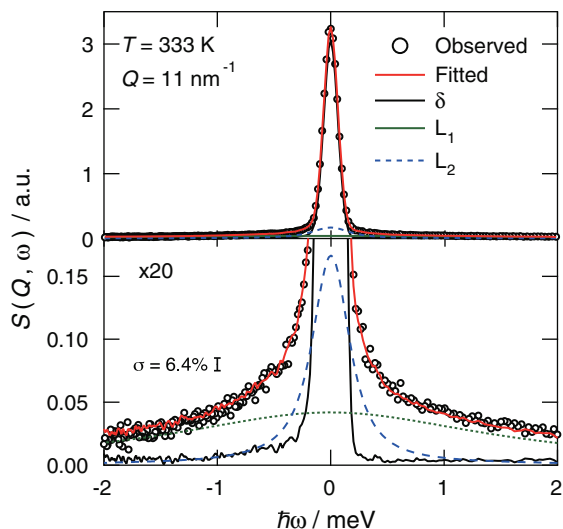


FIG. 9. Dynamic structure factors of d-C8mimCl observed at $Q = 11 \text{ nm}^{-1}$ and $T = 333 \text{ K}$. The curves are the results of the fitting. See text for the details.

be investigated by AGNES because limited number of detectors are installed at a low Q region in AGNES. We have tried to Fourier-transform the $S(Q, \omega)$ data on AGNES to $S(Q, t)$ data and superimpose them onto the NSE data, but it was unsuccessful since the energy range of AGNES is quite narrow and the data quality of AGNES is not very high.

D. Temperature dependence of relaxation times

Figure 10 shows the Arrhenius plot of the relaxation times obtained by NSE and AGNES. For the relaxation times determined by the stretched exponential (Kohlrausch-Williams-Watts) function, we plotted the averaged relaxation time $\langle \tau \rangle$ calculated from the relation $\langle \tau \rangle = \tau_{\text{KWW}}/\beta$, which is valid only for $\beta = 0.5$.³⁴ The viscosity data³⁵ of C8mimCl are also plotted for comparison. The scales for the relaxation

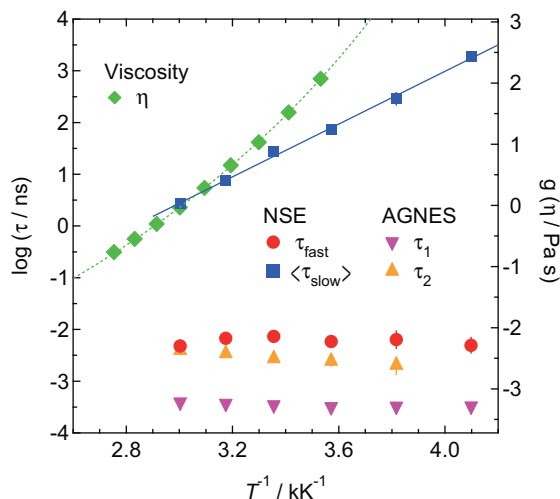


FIG. 10. Arrhenius plot of the relaxation times of d-C8mimCl observed on NSE and AGNES spectrometers. The viscosity data of C8mimCl (Ref. 35) are also plotted for comparison. Error bars represent standard uncertainty determined by the fitting.

time and viscosity were adjusted as in the Angell plot discussed frequently for glass-forming liquids.^{36,37}

We attribute the relaxations around 0.01 ns basically to the motions of the octyl-chain. This is because 11 nm^{-1} is near the Q value characteristic to the inter-alkyl correlation. Another evidence is our previous incoherent neutron scattering works on C4mimX ($X = \text{Cl, I, FeCl}_4, \text{TFSI}$).^{3,25} In each ionic liquid, an exponential relaxation appeared at around 1 ps at room temperature. Its activation energy is $\sim 15 \text{ kJ mol}^{-1}$, which is close to that of an intramolecular rotation of alkyl-chain, and does not depend on the anion X. These results suggest that the relaxation is due to the motion of the alkyl-chain connecting to an imidazolium ring. In the present data on d-C8mimCl, however, the relaxation times of the fast motions do not change much with temperature. This may be an artificial result caused by oversimplification of the fitting; i.e., the octyl-chain should have relaxation modes more than two. In such a case, it is expected that a mode with a relaxation time just matching the time scale of the spectrometer tends to be observed intensively and so the relaxation time determined by the fitting does not change much.

Another possibility of the mechanism of the fast relaxation is a “fast β relaxation” as suggested by Triolo *et al.*²² in their incoherent neutron scattering study on C4mimPF₆. Actually, the fast relaxation exhibits all characteristic properties of the fast β relaxation; i.e., an exponential decay, relaxation times of 1-10 ps, weak Q dependence of the relaxation time, and weak temperature dependence of the relaxation time. The problem of the fast β relaxation is that its microscopic origin is unknown though some people believe that it is a local relaxation in “cages” as predicted by the mode coupling theory.³⁸ Anyhow, more advanced experiments are required to make further discussion. One idea is an incoherent neutron scattering experiment with partially deuterated ionic liquids, e.g., comparing the relaxations among (C₈H₁₇)-(C₃N₂D₃)-CD₃, (C₈D₁₇)-(C₃N₂H₃)-CD₃, and (C₈D₁₇)-(C₃N₂D₃)-CH₃.

The relaxation times of the slow ionic motions obtained by NSE roughly agree with the viscosity data. This is reasonable since ionic motions should dominate the viscosity and be directly associated with the glass transition. The non-exponential parameter β is also close to the value ($\beta = 0.5$) for most of fragile glass-forming liquids. It is noteworthy that the NSE data look linear and tend to deviate from the viscosity data in the low temperature region. Such a relation between NSE and viscosity data was recognized also by Russina *et al.*²⁴ for C6mimTFSI and discussed in association with dielectric data and the Johari-Goldstein process of glass-forming liquids. The activation energy estimated from the NSE data is $(48.4 \pm 1.6) \text{ kJ mol}^{-1}$.

By assuming the Vogel-Tammann-Fulcher equation,^{39,40}

$$\tau = \tau_0 \exp\left(\frac{D}{T - T_0}\right), \quad (3)$$

and the definition of the fragility by Angell,^{36,37}

$$m = \left. \frac{d(\log \tau)}{d(T_g/T)} \right|_{T=T_g}, \quad (4)$$

the fragility m of C8mimCl is calculated to be 67.4 ± 0.1 by using the viscosity data and a part of the NSE data in the

high temperature region. This number is close to the values ($m = 71$) estimated by Russina *et al.*²⁴ Thus, the ionic liquids are as fragile as glass-forming molecular liquids; cf., $m = 80$ for orthoterphenyl and $m = 50$ for glycerol.^{36,37} This fact corresponds to large heat capacity jumps at glass transition temperatures of ionic liquids.^{2,3}

Finally, it should be noted that another motion, the domain relaxation, should exist in the time range longer than 100 ns. The observation of the domain relaxation is eagerly desirable to understand the overall feature of the dynamics of ILs.

IV. CONCLUSION

The present work has revealed the thermodynamic, structural and dynamic features of a typical ionic liquid C8mimCl. Heat capacity data demonstrated that C8mimCl exhibits a glass transition at $T_g = 214$ K, which is lower than T_g of C4mimCl with a shorter alkyl-chain. The neutron diffraction measurement for deuterated analogue d-C8mimCl revealed that the inter-ionic distance is insensitive to temperature while the packing of the alkyl-chains becomes more compact at low temperatures. The domain structure, which is specific to ionic liquids, becomes more vivid (ordered) and larger as decreasing temperature. The neutron quasielastic scattering data showed that C8mimCl has some faster relaxations probably corresponding to the combined motions of the octyl-group and a slower relaxation corresponding to the motion of ionic parts. The latter relaxation, which is related to the glass transition, is of non-exponential as in the α relaxation of glass-forming molecular liquids. The relaxation of domains could not be observed in the present experiment but should exist in the time range longer than 100 ns.

In order to make further discussion on the dynamics of ionic liquids, it is required to accumulate systematic quasielastic neutron scattering and viscosity data for various ionic liquids, including partially deuterated samples for neutron scattering. It should be interesting aspects how the fragility m and non-exponential parameter β depend on the length of alkyl-chain and the size of anions. It is, of course, important to investigate the domain motion using high energy-resolution spectrometers.

ACKNOWLEDGMENTS

This work is financially supported by the Grant-in-Aid for Scientific Research on Priority Area No. 17073004, MEXT, Japan. The work utilized facilities supported in part by the National Science Foundation under Agreement No. DMR-0944772.

Certain trade names and company products are identified in order to specify adequately the experimental procedure. In no case does such identification imply recommendation or endorsement by the National Institute of Standards and Technology, nor does it imply that the products are necessary the best for the purpose.

¹S. Hayashi and H. Hamaguchi, *Chem. Lett.* **33**, 1590 (2004).

²O. Yamamuro, Y. Minamimoto, Y. Inamura, S. Hayashi, and H. Hamaguchi, *Chem. Phys. Lett.* **423**, 371 (2006).

³O. Yamamuro, Y. Inamura, S. Hayashi, and H. Hamaguchi, *AIP Conf. Proc.* **832**, 73 (2006).

⁴K. Nakamura and T. Shikata, *ChemPhysChem* **11**, 285 (2010).

⁵K. Iwata, M. Kakita, and H. Hamaguchi, *J. Phys. Chem. B* **111**, 4914 (2007).

⁶H. Katayanagi, S. Hayashi, H. Hamaguchi, and K. Nishikawa, *Chem. Phys. Lett.* **392**, 460 (2004).

⁷K. Fujii, Y. Soejima, Y. Kyoshoin, S. Fukuda, R. Kanzaki, Y. Umebayashi, T. Yamamaguchi, S. Ishiguro, and T. Takamuku, *J. Phys. Chem. B* **112**, 4329 (2008).

⁸E. Bodo, L. Contrani, R. Caminti, N. V. Plechkova, K. R. Seddon, and A. Triolo, *J. Phys. Chem. B* **114**, 16398 (2010).

⁹C. S. Santos, H. V. R. Annapureddy, N. S. Murthy, H. K. Kashyap, E. W. Castner, Jr., and C. J. Margulis, *J. Chem. Phys.* **134**, 064501 (2011).

¹⁰C. S. Santos, N. S. Murthy, G. A. Baker, and E. W. Castner, Jr., *J. Chem. Phys.* **134**, 121101 (2011).

¹¹C. Hardacre, J. D. Holbrey, S. E. J. McMath, D. T. Bowron, and A. K. Soper, *J. Chem. Phys.* **118**, 273 (2003).

¹²A. Triolo, A. Mandanici, O. Russina, V. Rodrigues-Mora, M. Cutroni, C. Hardacre, M. Nieuwenhuyzen, H.-J. Bleif, L. Keller, and M. A. Ramos, *J. Phys. Chem. B* **110**, 21357 (2006).

¹³A. Triolo, O. Russina, H.-J. Bleif, and E. Di Cola, *J. Phys. Chem. B* **111**, 4641 (2005).

¹⁴A. Triolo, O. Russina, B. Fazio, R. Triolo, and E. Di Cola, *Chem. Phys. Lett.* **457**, 362 (2008).

¹⁵D. Xiao, L. G. Hines, Jr., S. Li, R. A. Bartsch, E. L. Quitevis, O. Russina, and A. Triolo, *J. Phys. Chem. B* **113**, 6426 (2009).

¹⁶C. Hardacre, J. D. Holbrey, C. L. Mullan, T. G. A. Youngs, and D. T. Bowron, *J. Chem. Phys.* **133**, 074510 (2010).

¹⁷Y. Wang and G. A. Voth, *J. Am. Chem. Soc.* **127**, 12192 (2005).

¹⁸J. N. A. C. Lopes and A. A. H. Padua, *J. Phys. Chem. B* **110**, 3330 (2006).

¹⁹H. V. R. Annapureddy, H. K. Kashyap, P. M. De Biase, and C. J. Margulis, *J. Phys. Chem. B* **114**, 16838 (2010).

²⁰S. Hayashi, R. Ozawa, and H. Hamaguchi, *Chem. Lett.* **32**, 498 (2003).

²¹S. Saha, S. Hayashi, A. Kobayashi, and H. Hamaguchi, *Chem. Lett.* **32**, 740 (2003).

²²A. Triolo, O. Russina, V. Arrighi, F. Juranyi, S. Janssen, and C. M. Gordon, *J. Chem. Phys.* **119**, 8549 (2003).

²³A. Triolo, O. Russina, C. Hardacre, M. Nieuwenhuyzen, M. A. Gonzalez, and H. Grimm, *J. Phys. Chem. B* **109**, 22061 (2005).

²⁴O. Russina, M. Beiner, C. Pappas, M. Russina, V. Arrighi, T. Unruh, C. L. Mullan, C. Hardacre, and A. Triolo, *J. Phys. Chem. B* **113**, 8469 (2009).

²⁵Y. Inamura, O. Yamamuro, S. Hayashi, and H. Hamaguchi, *Physica B* **385-386**, 732 (2006).

²⁶O. Yamamuro, M. Oguni, T. Matsuo, and H. Suga, *Bull. Chem. Soc. Jpn.* **60**, 1269 (1987).

²⁷K. Ohoyama, T. Kanouchi, K. Nemoto, M. Ohashi, T. Kajitani, and Y. Yamaguchi, *Jpn. J. Appl. Phys.* **37**, 3319 (1998).

²⁸N. Rosov, S. Rathgeber, and M. Monkenbusch, *ACS Symp. Ser.* **739**, 103 (2000).

²⁹M. Monkenbusch, R. Schätzler, and D. Richter, *Nucl. Instrum. Methods Phys. Res. A* **399**, 301 (1997).

³⁰R. T. Azuah, L. R. Kneller, Y. Qiu, P. L. W. Tregenna-Piggott, C. M. Brown, J. R. D. Copley, and R. M. Dimeo, *J. Res. Natl. Inst. Stand. Technol.* **114**, 341 (2009).

³¹T. Kajitani, K. Shibata, S. Ikeda, M. Kohgi, H. Yoshizawa, K. Nemoto, and K. Suzuki, *Physica B* **213-214**, 872 (1995).

³²O. Yamamuro, Y. Inamura, Y. Kawamura, S. Watanabe, T. Asami, and H. Yoshizawa, *Annual Report of Neutron Science Laboratory* (Institute for Solid State Physics, University of Tokyo, 2005), Vol. 12, p. 2.

³³G. W. Stewart, *Phys. Rev.* **31**, 174 (1928).

³⁴C. P. Lindsey and G. D. Patterson, *J. Chem. Phys.* **73**, 3348 (1980).

³⁵K. R. Seddon, A. Stark, and M.-J. Torres, *ACS Symp. Ser.* **819**, 34 (2002).

³⁶C. A. Angell, *J. Phys. Chem. Solids* **49**, 863 (1988).

³⁷C. A. Angell, *J. Non-Cryst. Solids* **131-133**, 13 (1991).

³⁸For example, B. Frick and D. Richter, *Science* **267**, 1939 (1995); U. Buchenau, in *Dynamics of Disordered Materials*, edited by D. Richter, A. J. Dianoux, W. Petry, and J. Teixeira (Springer-Verlag, Berlin, 1989).

³⁹H. Vogel, *Phys. Z.* **22**, 645 (1922).

⁴⁰G. S. Fulcher, *J. Am. Chem. Soc.* **8**, 339 (1925).